The *nn* quasifree *nd* breakup cross section: Discrepancies with theory and implications for the $^1S_0$ *nn* force

H. Witała
M. Smoluchowski Institute of Physics, Jagiellonian University, PL-30059 Kraków, Poland

W. Glöckle
Institut für theoretische Physik II, Ruhr-Universität Bochum, D-44780 Bochum, Germany
(Received 21 November 2010; published 11 March 2011)

Large discrepancies between quasifree neutron-neutron (*nn*) cross section data from neutron-deuteron (*nd*) breakup and theoretical predictions based on standard nucleon-nucleon (*NN*) and three-nucleon (3*N*) forces are pointed out. The *nn* $^1S_0$ interaction is shown to be dominant in that configuration and has to be increased to bring theory and data into agreement. Using the next-to-leading order $^1S_0$ interaction of chiral perturbation theory, we demonstrate that the *nn* quasifree scattering cross section depends only slightly on changes of the *nn* scattering length but is very sensitive to variations of the effective range parameter. In order to account for the reported discrepancies one must decrease the *nn* effective range parameter by ≈12% from its value implied by charge symmetry and charge independence of nuclear forces.

DOI: 10.1103/PhysRevC.83.034004 PACS number(s): 21.45.Bc, 21.30.Fe, 25.10.+s, 25.40.Cm

I. INTRODUCTION

The knowledge of the nucleon-nucleon (*NN*) interaction is fundamental for interpreting nuclear phenomena. Proton-proton (*pp*) experiments provide a solid data basis [1,2], which restricts theoretical assumptions about the strong part of the *pp* force. In the case of the neutron-proton (*np*) system this is true only to a smaller extent. The partial wave analysis of the *np* data [2] relies on the assumption that the isospin $t = 1$ piece can be taken over from the *pp* system and only the $t = 0$ part is free in the adjustment to the data. The lack of a free neutron target forbids neutron-neutron (*nn*) experiments, therefore information on the *nn* interaction can be deduced only in an indirect way. To that aim the best tool seems to be the study of the three-nucleon (3*N*) system composed of two neutrons and the proton. It is simple enough to allow a rigorous theoretical treatment, e.g., in the framework of Faddeev equations [3]. The neutron-deuteron elastic scattering together with the neutron-induced deuteron breakup, supplemented with the triton properties, offer a data basis that can be used to test properties of the *nn* force. In particular, the *nd* breakup process with its rich set of configurations for three free outgoing nucleons seems to be a powerful tool to test the nuclear Hamiltonian. By comparing theoretical predictions to the *nd* breakup data in different configurations not only can the present-day models of two-nucleon (2*N*) interactions be tested, but also the effects of three-nucleon forces (3NF's) can be studied.

nn quasifree scattering (QFS) refers to a situation where the outgoing proton is at rest in the laboratory system. In *nd* breakup *np* QFS is also possible. Here one of the neutrons is at rest while the second neutron together with the proton forms a quasifreely scattered pair.

The reported *nn* QFS cross sections taken at $E_n^{\rm lab} = 26$ [4] and 25 MeV [5] overestimate the *nd* theory by ≈18%. Surprisingly, when instead of the *nn* pair the *np* pair is quasifreely scattered, the theory follows nicely the *np* QFS cross section data taken in the $E_n^{\rm lab} = 26$ MeV *nd* breakup measurement [4]. That good description of the *np* QFS cross section contrasts with the drastic discrepancy between the theory and the *nn* QFS cross section data taken in the same experiment [4].

We do not expect surprises in the case of the *pp* QFS data [6–8], since the information from the rich set of *pp* data has been incorporated into the *pp* forces. In fact a recent analysis [9] including the Coulomb force in the *pp* QFS data led to a nice agreement, while in previous analyses [6–8] the Coulomb force was not yet included. Additional theoretical efforts to include all effects of the Coulomb force beyond the ones in [9] are under way.

In Sec. II we exemplify the stability of the QFS cross sections against changes of modern nuclear forces. We also demonstrate that below ≈30 MeV the $^1S_0$ and $^3S_1$-$^3D_1$ *NN* force components dominate the QFS cross sections. In Sec. III we analyze the *np* as well as the *nn* QFS data from [4] in terms of rigorous solutions of the 3*N* Faddeev equation and discuss necessary changes in the $^1S_0$ *nn* force component to remove the discrepancies in the *nn* QFS cross section. There a detailed study is performed using the next-to-leading order (NLO) chiral *NN* force, composed of contact interactions and the one- and two-pion exchange terms. It reveals that the effective range parameter is decisive to reconcile theory and data. The outcome is discussed in Sec. IV and further experimental insights into the *nn* force are proposed. Finally we summarize in Sec. V.

II. STABILITY AND SENSITIVITY STUDIES

It is known that *nd* scattering theory provides QFS cross sections that are highly independent of the realistic *NN* potential used in the calculations and that they essentially do not change when any of the present day 3NF's is included [3,10,11]. We exemplify this in Fig. 1 for the *nn* and *np*

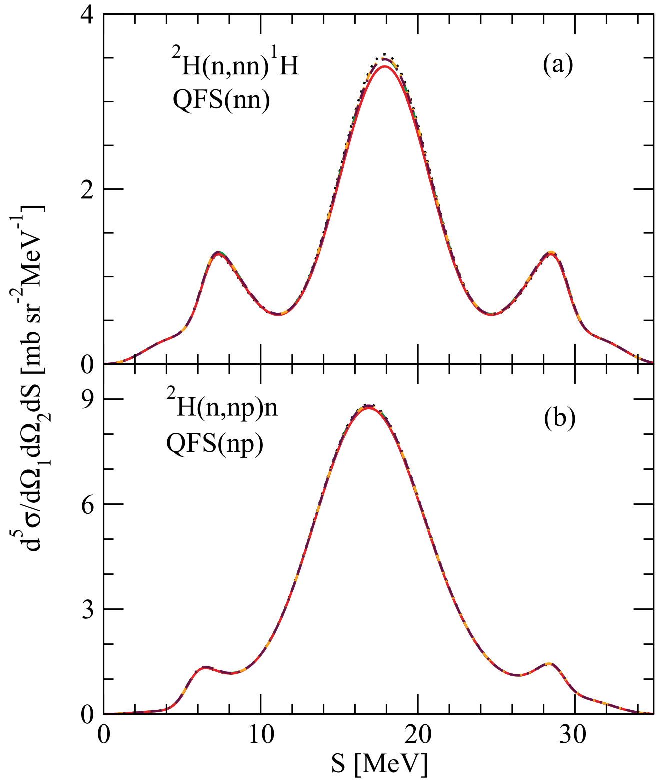

FIG. 1. (Color online) The cross section $d^5\sigma/d\Omega_1 d\Omega_2 dS$ for the $E_n^{\rm lab} = 26$ MeV *nd* breakup reactions ^{2}H$(n,nn)^1$H (a) and ^{2}H$(n,np)n$ (b) as a function of the S-curve length for two complete configurations of Ref. [4]. QFS *nn* refers to the angles of the two neutrons, $\theta_1 = \theta_2 = 42^\circ$, and QFS *np* refers to the angle $\theta_1 = 39^\circ$ of the detected neutron and $\theta_2 = 42^\circ$ for the proton. In both cases $\phi_{12} = 180^\circ$. The (practically overlapping) lines correspond to different underlying dynamics: CD Bonn [13], dashed (blue); Nijm I, dotted (black); Nijm II [14], dash-dotted (green); CD Bonn + TM99, solid (red); Nijm I + TM99 [15,16], dash-double-dotted (orange); Nijm II + TM99, double-dash-dotted (maroon). All partial waves with 2*N* total angular momenta up to $j_{\rm max} = 5$ have been included.

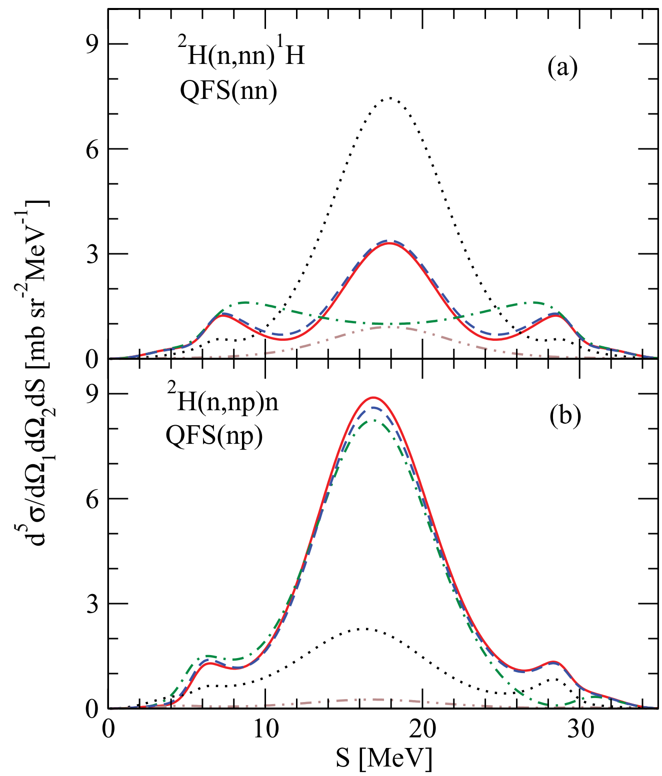

FIG. 2. (Color online) The cross section $d^5\sigma/d\Omega_1 d\Omega_2 dS$ for the $E_n^{\rm lab} = 26$ MeV *nd* breakup reactions ^{2}H$(n,nn)^1$H (a) and ^{2}H$(n,np)n$ (b) as a function of the S-curve length for two complete configurations of Ref. [4] specified in Fig. 1. The different lines show contributions from different *NN* force components. The solid (red) line is the full result based on the CD Bonn potential [13] and all partial waves with 2*N* total angular momenta up to $j_{\rm max} = 5$ included. The dotted (black), dash-dotted (green), and dashed (blue) lines result when only contributions from $^1S_0$, $^3S_1$-$^3D_1$, and $^1S_0$ + $^3S_1$-$^3D_1$ are kept in calculating the cross sections. The dash-double-dotted (brown) line presents the contribution of all partial waves with the exception of $^1S_0$ and $^3S_1$-$^3D_1$.

QFS geometries of Ref. [4]. There the results of 3*N* Faddeev calculations [3] based on different-high precision *NN* forces (CD Bonn [13], Nijm I and Nijm II [14]) alone or combined with the TM99 3NF [15,16] are shown.

The sensitivity study performed in [10] revealed that at energies below ≈30 MeV the $^1S_0$ and $^3S_1$-$^3D_1$ *NN* force components provide the most dominant contribution to the QFS cross sections with much smaller contributions of higher partial waves. Specifically, in the *np* QFS geometries the $^3S_1$-$^3D_1$ is the dominant force component while for *nn* QFS it is the $^1S_0$ force that contributes decisively. Again we exemplify it for the *nn* and *np* QFS geometries of Ref. [4] in Fig. 2. Such a dominance for the QFS peak is understandable since the QFS cross sections are almost insensitive to the action of the presently available 3NF. Then at low energy the largest contribution should be provided by the *S*-wave components of the *NN* potential. In the cases of free *np* and *nn* scattering these are the $^1S_0(np) + ^3S_1$-$^3D_1$ and $^1S_0(nn)$ contributions, respectively. In the simple-minded spirit that under QFS conditions one of the three nucleons (at rest in the laboratory system) is just a spectator, such a dominance of a two-nucleon encounter is to be expected. In reality, however, the projectile nucleon also interacts with that "spectator" particle and the three nucleons at low energies undergo higher-order rescatterings [3,12]. Thus the scattering to the final *nn* (*np*) QFS configuration also receives contributions from the *np* $^3S_1$-$^3D_1$ (*nn* $^1S_0$) interaction. Despite all that, the numerical results clearly reveal that for the *np* QFS configuration the $^3S_1$-$^3D_1$ force is the most dominant contribution and for the *nn* QFS it is the $^1S_0$ force (for free *nn* scattering there is no $^3S_1$-$^3D_1$ interaction possible). This implies that the *nn* QFS is a powerful tool to study the $^1S_0$ *nn* force component.

That extreme sensitivity of the *nn* QFS cross section to the $^1S_0$ *nn* force component is demonstrated in Fig. 3 for the QFS geometries of Ref. [4]. With that aim we multiplied the $^1S_0$ *nn* matrix element of the CD Bonn potential by a factor of λ. The result is that the *nn* QFS cross section undergoes significant variations while the *np* QFS cross section is practically unchanged. The displayed λ parameters include

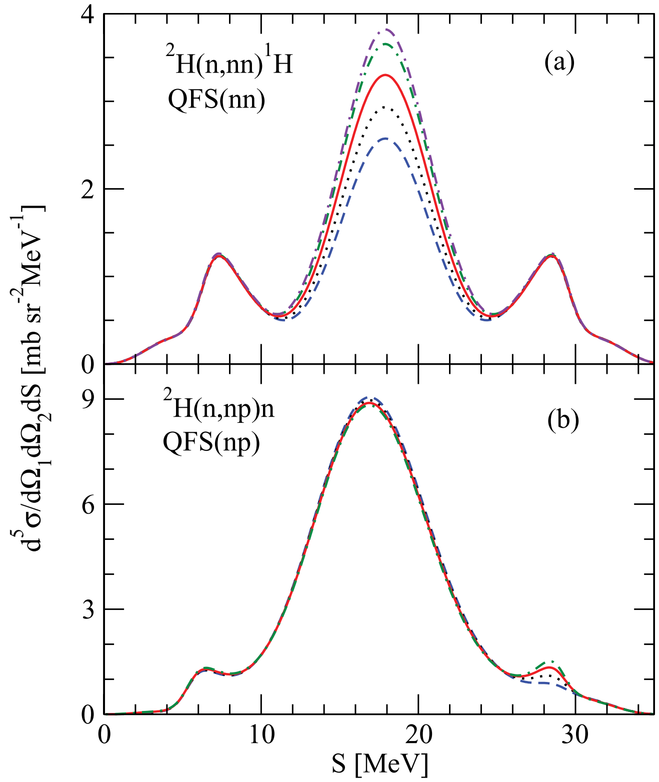

FIG. 3. (Color online) The cross section $d^5\sigma/d\Omega_1 d\Omega_2 dS$ for the $E_n^{\rm lab} = 26$ MeV *nd* breakup reactions ^{2}H$(n,nn)^1$H (a) and ^{2}H$(n,np)n$ (b) as a function of the S-curve length for two complete configurations of Ref. [4] specified in Fig. 1. The lines show sensitivity of the QFS cross sections to the changes of the *nn* $^1S_0$ force component. Those changes were induced by multiplying the $^1S_0$ *nn* matrix element of the CD Bonn potential by a factor λ. The solid (red) line is the full result based on the original CD Bonn potential [13] ($a_{nn} = -18.8$ fm, $r_{\rm eff} = 2.79$ fm) and all partial waves with 2*N* total angular momenta up to $j_{\rm max} = 5$ included. The dashed (blue), dotted (black), and dash-dotted (green) lines correspond to $\lambda = 0.9$ ($a_{nn} = -8.3$ fm, $r_{\rm eff} = 3.12$ fm), 0.95 ($a_{nn} = -11.7$ fm, $r_{\rm eff} = 2.96$ fm), and 1.05 ($a_{nn} = -42.0$ fm, $r_{\rm eff} = 2.66$ fm), respectively. The double-dash-dotted (violet) line shows cross sections obtained with $\lambda = 1.08$ ($a_{nn} = -134.7$ fm, $r_{\rm eff} = 2.61$ fm), which factor is required to get agreement with *nn* QFS data of Ref. [4].

also the value $\lambda = 1.08$ which is necessary to get agreement with the *nn* QFS data of Ref. [4].

While both $^1S_0$ and $^3S_1$-$^3D_1$ *np* forces are well determined by *np* scattering data (with the restrictions mentioned above) and by the deuteron properties, the $^1S_0$ *nn* force is determined up to now only indirectly owing to lack of free *nn* data. The disagreement between data and theory in the *nn* QFS peak points to the possibility of a flaw in the *nn* $^1S_0$ force. It was shown in [10] that removal of the ≈18% discrepancy found in [4] for the *nn* QFS cross section required an increased strength of the $^1S_0$ *nn* interaction which when given in terms of a factor λ amounts to $\lambda \approx 1.08$. In Fig. 4 we show the effect of the λ modification for the *nn* scattering length a_{nn} and for the effective range parameter $r_{\rm eff}$, and in Fig. 5 for the binding energy of two neutrons in the $^1S_0$ state. It is seen that taking $\lambda = 1.08$ leads to a nearly bound state of two neutrons.

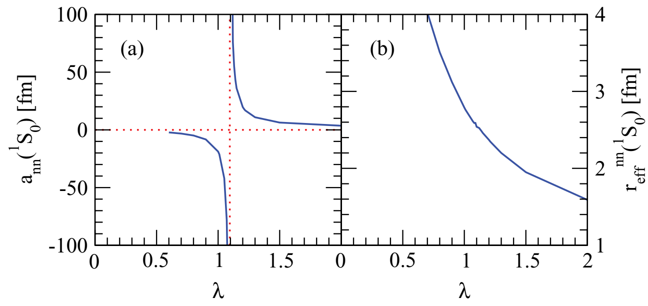

FIG. 4. (Color online) The changes of the *nn* scattering length a_{nn} (a) and the effective range parameter $r_{\rm eff}$ (b) with factor λ by which the $^1S_0$ *nn* matrix element of the CD Bonn potential is multiplied: $V_{nn}(^1S_0) = \lambda V_{\rm CDBonn}(^1S_0)$.

III. IMPLICATIONS FOR THE $^1S_0$ *NN* EFFECTIVE RANGE PARAMETER

Since the multiplication of the $^1S_0$ potential matrix element by a factor λ induces changes in the effective range as well as in the scattering length, the question arises as to which of the two effects is more important for the *nn* QFS cross section variations. To answer that question we performed 3*N* Faddeev calculations based on the next-to-leading order ciral perturbation theory (χPT) potential [17,18] including all *np* and *nn* forces up to the total angular momentum $j_{\rm max} = 3$ in the two-nucleon subsystem. The $^1S_0$ component of that interaction is composed of the one- and two-pion exchange terms and contact interactions parametrized by two parameters $\tilde{C}_{^1S_0}$ and $C_{^1S_0}$,

$$V(^1S_0) = \tilde{C}_{^1S_0} + C_{^1S_0}(p^2 + p'^2). \tag{1}$$

Standard values are $\tilde{C}_{^1S_0} = -0.155\,737\,4 \times 10\,000$ GeV^{-2} and $C_{^1S_0} = 1.507\,522\,0 \times 10\,000$ GeV^{-4} for cutoff combinations $\{\Lambda, \tilde{\Lambda}\} = \{450$ MeV, 500 MeV$\}$ [18].

By multiplying $\tilde{C}_{^1S_0}$ by a factor $C_2(^1S_0)$ and $C_{^1S_0}$ by a factor $C_1(^1S_0)$, one can induce changes of the *nn* $^1S_0$ interaction. The requirement that either the value of the scattering length a_{nn}

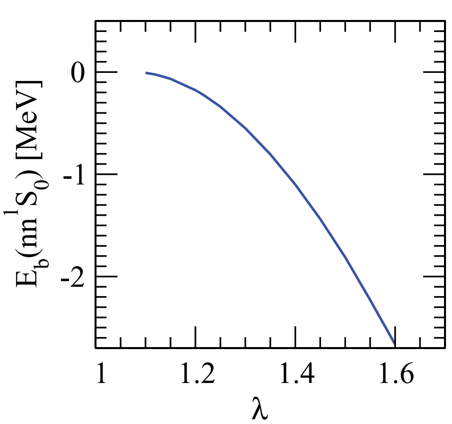

FIG. 5. (Color online) The range of λ values by which the $^1S_0$ *nn* matrix element of the CD Bonn potential is multiplied [$V_{nn}(^1S_0) = \lambda V_{\rm CDBonn}(^1S_0)$], for which the two neutrons form a bound state with the binding energy E_b.

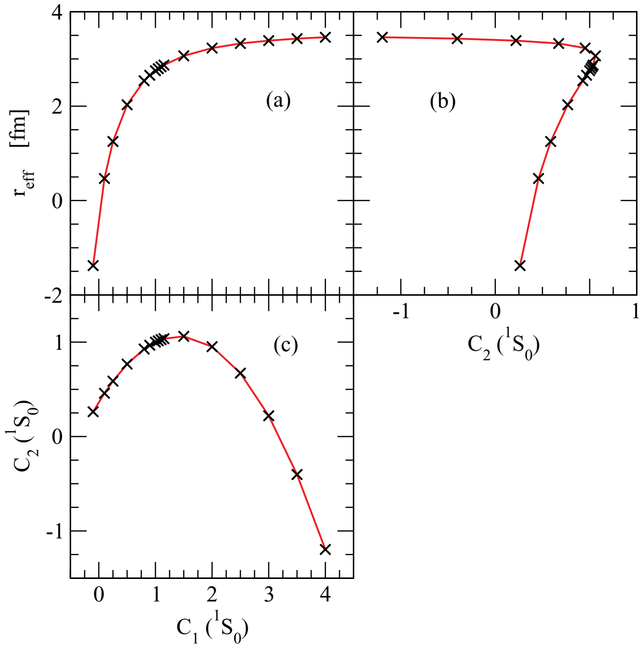

FIG. 6. (Color online) Changes of the effective range parameter $r_{\rm eff}$ in the $^1S_0$ partial wave (a) and (b) caused by a correlated change of the factors $C_1(^1S_0)$ and $C_2(^1S_0)$ shown in (c). This correlation between the factors $C_1(^1S_0)$ and $C_2(^1S_0)$ corresponds to a constant value of the scattering length $a_{nn} = -17.6$ fm.

or the value of the effective range parameter $r_{\rm eff}$ be constant correlates the $C_1(^1S_0)$ and $C_2(^1S_0)$ factors.

Changing $C_1(^1S_0)$ and $C_2(^1S_0)$ in such a way that the scattering length is kept constant and equal to $a_{nn} = -17.6$ fm leads to changes of the effective range $r_{\rm eff}$ shown in Fig. 6. The resulting changes of the *nn* and *np* QFS cross sections for the geometries of Ref. [4] are shown in Fig. 7 for five sets of $C_1(^1S_0)$ and $C_2(^1S_0)$ factors with different *nn* $^1S_0$ effective range parameters ranging from $r_{\rm eff} = 2.03$ to 3.07 fm; one of them corresponds to the value required by the data.

Similarily, changing $C_1(^1S_0)$ and $C_2(^1S_0)$ while keeping the effective range constant to $r_{\rm eff} = 2.75$ fm leads to changes of the *nn* $^1S_0$ scattering length a_{nn} shown in Fig. 8. The resulting changes of the *nn* and *np* QFS cross sections are presented in Fig. 9 for four values of the *nn* $^1S_0$ scattering length ranging from $a_{nn} = -10.9$ to -75.9 fm. It is clearly seen that the *nn* QFS cross sections depend only slightly on a change of the scattering length. The variation of the QFS cross section maximum stays below $\approx\pm 4\%$. In contrast, much stronger variations of the *nn* QFS cross sections result from changes of the effective range (see Fig. 7).

Thus we can conclude that the λ enhancement mechanism for the $^1S_0$ *nn* force studied in [10] acts mainly through the change of the effective range parameter. Thus in order to remove the discrepancies found in [4] and [5] for the *nn* QFS cross section, a change of the *nn* $^1S_0$ effective range parameter is required. Its value taken under the assumption of charge symmetry and charge independence of nuclear forces is $r_{\rm eff} = 2.75$ fm and it has to be changed to $r_{\rm eff} \approx 2.41$ fm. That implies a large charge-symmetry- and charge-independence-breaking effect of about $\approx 12\%$ for that parameter.

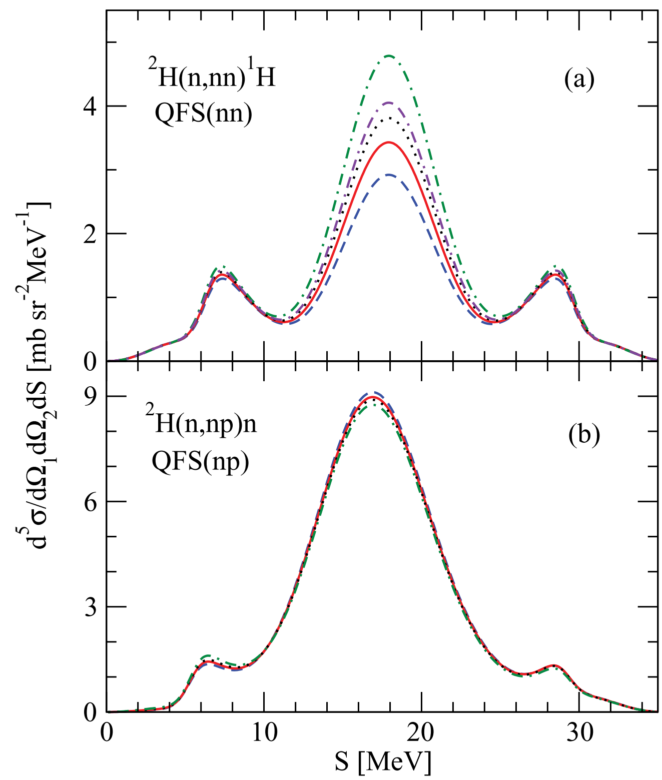

FIG. 7. (Color online) Changes of QFS cross sections for configurations specified in Fig. 1 caused by correlated change of factors $C_1(^1S_0)$ and $C_2(^1S_0)$ shown in Fig. 6. All lines show results of Faddeev calculations based on NLO χPT potential and all partial waves with 2*N* total angular momenta up to $j_{\rm max} = 3$ included. They differ in the *nn* $^1S_0$ force which was obtained keeping constant the scattering length $a_{nn} = -17.6$ fm and changing the constants $C_1(^1S_0)$ and $C_2(^1S_0)$ to get different effective ranges as follows: solid (red line), $C_1(^1S_0) = 1.0$, $C_2(^1S_0) = 1.0$, $r_{\rm eff} = 2.75$ fm; dashed (blue line), $C_1(^1S_0) = 1.5$, $C_2(^1S_0) = 1.0615$, $r_{\rm eff} = 3.07$ fm; dotted (black line), $C_1(^1S_0) = 0.8$, $C_2(^1S_0) = 0.9275$, $r_{\rm eff} = 2.54$ fm; dash-dotted (green line), $C_1(^1S_0) = 0.5$, $C_2(^1S_0) = 0.7675$, $r_{\rm eff} = 2.03$ fm. The double-dash-dotted (violet) line shows cross sections obtained with $C_1(^1S_0) = 0.7064$, $C_2(^1S_0) = 0.8842$, $r_{\rm eff} = 2.41$ fm, which are required to get agreement with *nn* QFS data of Ref. [4].

We would like to add that the discussed changes of $r_{\rm eff}$ did not affect the elastic *nd* cross section nor the vector or tensor analyzing powers to a measurable extent. Only more complicated spin observables in elastic *nd* scattering are affected but the present-day experimental errors are much larger than those changes. Of special interest for the *nd* breakup reaction is a region of phase space around a final-state-interaction (FSI) geometry, where two of the three outgoing nucleons have equal and parallel momenta. Because of their their large sensitivity to the $^1S_0$ scattering length, FSI cross sections were always considered as a useful tool to extract that quantity. Therefore the question arises as to what extent a large change of the *nn* $^1S_0$ effective range, required to bring theory into agreement with the QFS *nn* cross section data, influences the FSI cross sections? It turns out that for such large changes of the effective range parameter the FSI cross sections depend not only on the scattering length but also on the effective range.

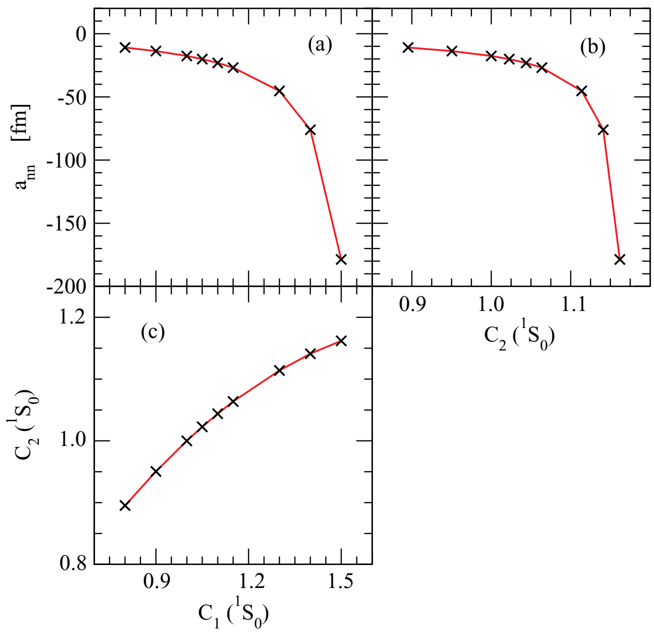

FIG. 8. (Color online) Changes of the *nn* scattering length a_{nn} in the $^1S_0$ partial wave (a) and (b) caused by a correlated change of the factors $C_1(^1S_0)$ and $C_2(^1S_0)$ as shown in (c). This correlation between the factors $C_1(^1S_0)$ and $C_2(^1S_0)$ corresponds to a constant value of the effective range parameter $r_{\rm eff} = 2.75$ fm.

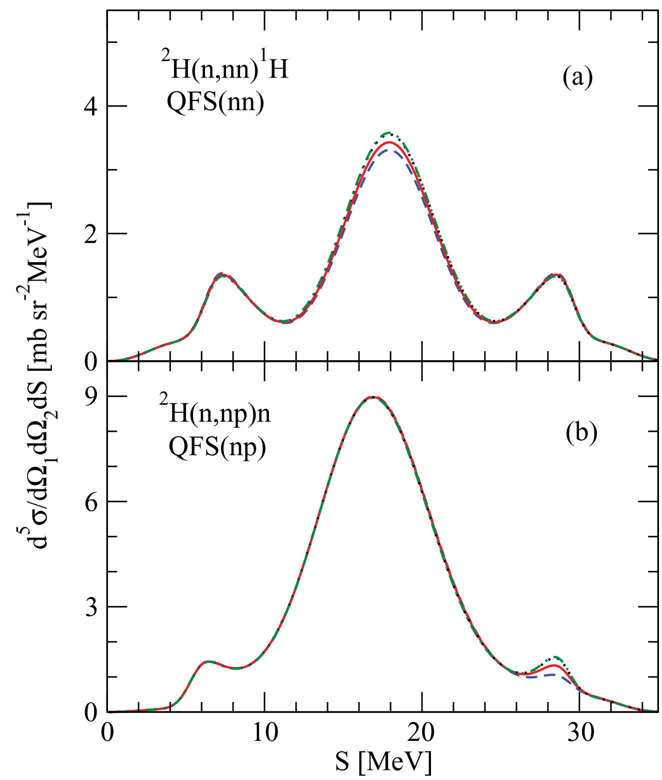

FIG. 9. (Color online) Changes of QFS cross sections for configurations specified in Fig. 1 caused by a correlated change of the factors $C_1(^1S_0)$ and $C_2(^1S_0)$ shown in Fig. 8. All lines show results of Faddeev calculations based on the NLO χPT potential and all partial waves with 2*N* total angular momenta up to $j_{\rm max} = 3$ included. They differ in the *nn* $^1S_0$ force which was obtained keeping the effective range parameter $r_{\rm eff} = 2.75$ fm constant and changing the constants $C_1(^1S_0)$ and $C_2(^1S_0)$ to get different scattering lengths as follows: solid (red line), $C_1(^1S_0) = 1.0$, $C_2(^1S_0) = 1.0$, $a_{nn} = -17.6$ fm; dashed (blue line), $C_1(^1S_0) = 0.8$, $C_2(^1S_0) = 0.8953$, $a_{nn} = -10.9$ fm; dotted (black line), $C_1(^1S_0) = 1.3$, $C_2(^1S_0) = 1.1139$, $a_{nn} = -45.3$ fm; dash-dotted (green line), $C_1(^1S_0) = 1.4$, $C_2(^1S_0) = 1.1410$, $a_{nn} = -76.0$ fm.

The above change of $r_{\rm eff}$ leads, depending on the outgoing angle of the final-state interacting *nn* pair, to changes of the *nn* FSI cross sections up to about ≈25%. However, it leads to a much smaller variations of the *np* FSI cross sections, which for the outgoing angles of the *np* final-state interacting pair in the range $30^\circ \leqslant \theta_{\rm lab} \leqslant 50^\circ$ are under 5%. In view of that, it seems that in order to provide a reliable value of the *nn* scattering length, any analysis of the *nn* FSI cross sections should be based on a reliable value of the *nn* effective range parameter.

Since the $^1S_0$ *NN* force component contributes to the binding energy of the triton, the changes of that force in the *nn* subsystem will lead to variations of the triton binding energy. Specifically, the above change of the effective range leads to an increase of the ^{3}H binding by 0.7 MeV. Such a variation of the binding energy can be easily compensated by the effects of three-nucleon forces.

IV. DISCUSSION AND FURTHER EXPERIMENTAL INFORMATION

Is such a large isospin breaking effect at all possible in view of the present understanding of nuclear forces? First, it seems improbable that only the effective range will reveal large isospin breaking and the scattering length will be left unaffected. In χPT the leading isospin breaking contribution is provided by the isospin breaking contact interaction without derivatives [19]. It turns out that the effective range parameter is quite insensitive to that isospin breaking contact force, and typical isospin breaking effects for $r_{\rm eff}$ are small, under ≈1% [19].

The reported discrepancies for *nn* QFS require, however, a much larger effect for $r_{\rm eff}$, of the order of ≈12%. Only when the contact terms in next orders would be unnaturally large could one expect larger isospin breaking effects for $r_{\rm eff}$. Assuming naturalness, this seems rather improbable.

Since it seems unlikely that isospin breaking effects will show up, if at all, in the effective range parameter alone without affecting simultaneously the *nn* scattering length, the question of the possible existence of a bound state of two neutrons reappears. Present-day *NN* interactions allow only one bound state of two nucleons, namely, the deuteron, where the neutron and the proton are interacting in a state with angular momentum $l = 0$ or 2, total spin $s = 1$, and total angular momentum $j = 1$. When the neutron and proton are interacting with the $^1S_0$ force no bound state exists and only a virtual resonant state occurs, as documented by the negative scattering length $a_{np} = -21.73$ fm. The data for the proton-proton system also exclude a $^1S_0$ *pp* bound state; however, in this case the nuclear force is overpowered by

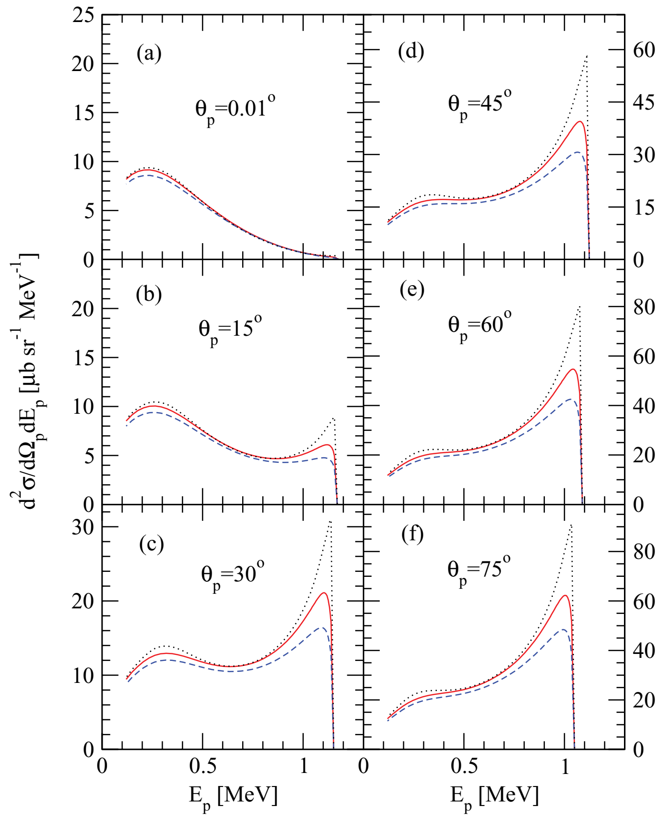

FIG. 10. (Color online) The spectra of the outgoing proton from the reaction ^{3}H$(\gamma,p)nn$ with $E_\gamma = 10$ MeV at different laboratory angles of the proton. They have been calculated using the AV18 [25] *NN* interaction and a current composed of single nucleon and meson exchange currents [26]. The solid (red) line is based on the AV18 potential ($a_{nn} = -18.8$ fm, $r_{\rm eff} = 2.83$ fm). The dotted (black) and dashed (blue) lines show sensitivity of the spectra to changes of the *nn* $^1S_0$ force component used in the 3*N* continuum part of the calculations. Those changes were induced by multiplying the $^1S_0$ *nn* matrix element of the AV18 potential by a factor λ. For the dotted and dashed lines $\lambda = 1.05$ ($a_{nn} = -54.3$ fm, $r_{\rm eff} = 2.67$ fm) and 0.95 ($a_{nn} = -10.9$ fm, $r_{\rm eff} = 3.02$ fm), respectively.

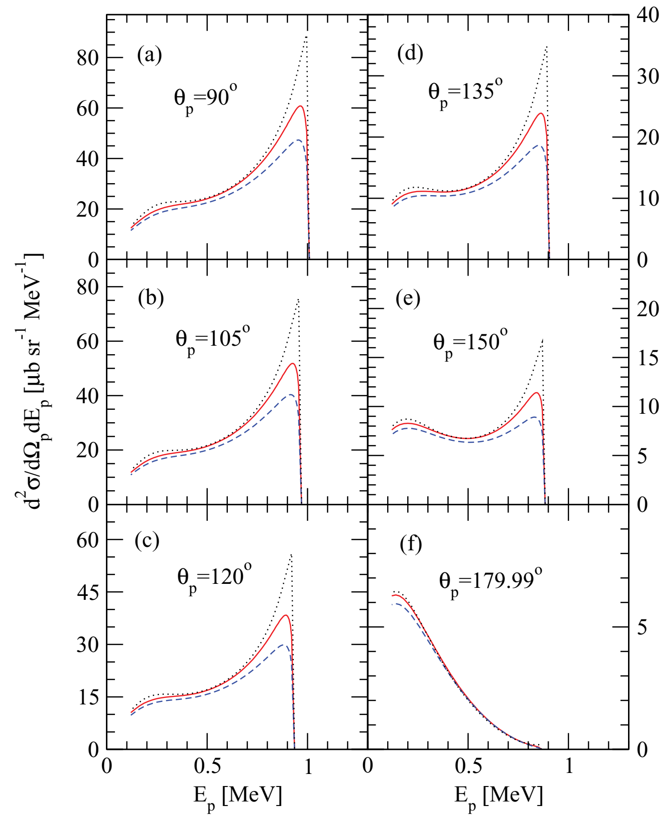

FIG. 11. (Color online) The spectra of the outgoing proton from the reaction ^{3}H$(\gamma,p)nn$ with $E_\gamma = 10$ MeV at different laboratory angles of the proton. They have been calculated using the AV18 [25] *NN* interaction and a current composed of single nucleon and meson exchange currents [26]. For explanation of lines, see Fig. 10.

the strong *pp* Coulomb repulsion. Also, assuming charge independence and charge symmetry of strong interactions the two neutrons should not bind in the $^1S_0$ state.

It also seems that modern nuclear forces do not allow for the 3*n* and 4*n* systems to be bound [20]. However, in view of the strong discrepancies between theory and data found in the *nd* breakup measurements for the *nn* QFS geometry, which cannot be explained by present-day nuclear forces, it appears reasonable to check experimentally the possibility of two neutrons being bound.

There are reactions that provide conditions advantageous for a hypothetical dineutron bound state. Such conditions can be found, e.g., when two neutrons are moving with equal momenta and with relative energy close to zero. That occurs in the so-called final-state-interaction geometry of *nd* breakup. Incomplete *nd* breakup measurements have been performed in the past to study properties of the $^1S_0$ *nn* force [21]. A dedicated experiment was even performed in order to look for a hypothetical $^1S_0$ *nn* bound state [22] in which the spectrum of the proton going in the forward direction was measured with the aim of a precise determination of its high-energy region. The negative result of [22] showed that the *nd* reaction is not suitable for such a study.

It seems that much more appropriate would be reactions in which from the beginning two neutrons occupy a configuration advantageous for their binding. It is known [23,24] that ^{3}He is predominantly a spatially symmetric *S* state with its two protons mainly in opposite spin states. This component amounts for ≈90% of the ^{3}He wave function. Similarly, the two neutrons in ^{3}H are restricted to be in a spin-singlet state. That makes the triton target a very suitable tool to look for a *nn* bound state in γ-induced breakup of ^{3}H. The idea is to measure the spectra of the outgoing protons in such a reaction. The two-neutron bound state, if it exists, should reveal itself as a peak above the highest available proton energy from the three-body decay of ^{3}H. We show in Figs. 10 and 11 the outgoing proton spectra from the $\gamma(^3H,p)nn$ reaction for a number of γ energies and angles of the outgoing protons. These spectra have been calculated using the AV18 [25] *NN* interaction and a current composed of single nucleon and meson exchange currents [26]. We demonstrate in Figs. 10 and 11 the large sensitivity of the high-energy part of these spectra to changes of the $^1S_0$ *nn* interaction. That is, the dashed and dotted lines resulted when we multiplied the $^1S_0$ *nn* matrix element of the AV18 potential by a factor λ and used it in the 3N continuum part of the calculations. Such modifications of the $^1S_0$ *nn* interaction lead to significant changes of the higher-energy part of the spectra. The big advantage of that reaction is that the γ interacts predominantly with the proton.

Other reactions, such as, e.g., ^{3}H(n,d)nn and ^{3}H(d,^{3}He)nn, also provide conditions advantageous for the binding of two neutrons. They are complementary to and independent of the ^{3}H(γ,p)nn reaction, and the data from all three processes should provide an answer to the question of whether two neutrons can form a bound state. The reaction ^{3}H(d,^{3}He)nn cannot presently be treated in a theoretically rigorous manner, but with the rapid increase in computer power such a treatment based on Fadeev-Yakubovsky equations can be expected in the near future.

V. SUMMARY

The strong discrepancy in the *nn* QFS *nd* breakup configuration found in [4,5] is reconsidered. It is documented again that at low energies (below ≈30 MeV) the *nn* (*np*) QFS cross section depends predominantly only on the $^1S_0$ ($^3S_1$-$^3D_1$) *NN* force component and higher-partial-wave contributions are quite small. Furthermore the theoretical results are quite stable under exchange of the standard nuclear forces. Also the presently available 3*N* forces have negligible effect on the QFS configurations. Since no direct measurement of the *nn* force is available, there is the possibility that the properties of the *nn* force are still unsettled. Thus by simply multiplying the *nn* $^1S_0$ force matrix element by a factor $\lambda = 1.08$ one can perfectly well reconcile theory and data. In addition we performed a more detailed study using the NLO chiral potential, which is composed of the one- and two-pion exchange and contact interactions depending on two parameters. That dependence allowed us to study separately variations in the scattering length a_{nn}, leaving the effective range parameter $r_{\rm eff}$ constant, and vice versa. Thereby it turned out that the *nn* QFS peak height is very sensitive to $r_{\rm eff}$ and hardly sensitive to a_{nn}. The outcome for an agreement with the data is the requirement that $r_{\rm eff}$ decreases from the value $r_{\rm eff} = 2.75$ fm to a significantly smaller one, $r_{\rm eff} = 2.41$ fm. That strongly breaks charge symmetry and charge independence and is not supported by present-day chiral potential theory. In that context, however, the charge-independence- and charge-symmetry-breaking $2\pi\gamma$ long-range *NN* interactions [27] might be of interest, too.

So, what might be a solution to remove the discrepancy? If the data are taken for granted there remains the possibility that a di-neutron exists. We propose additional experimental investigations, of, for instance, the $^3H(\gamma,p)nn$ process, and evaluatation of the proton spectra at various emission angles emphasizing the high-energy region.

The direct inclusion of Δ degrees of freedom into χPT allows for a rich set of additional *NN* and 3*N* force diagrams which are presently under investigation [28]. This might reconcile theory and data also for the space-star discrepancy [3] in the *nd* breakup process. Right now the situation is unsettled.

ACKNOWLEDGMENTS

This work was supported by the Polish science funds as the Research Project No. N N202 077435. It was also partially supported by the Helmholtz Association through funds provided to the virtual institute "Spin and strong QCD" (Grant No.VH-VI-231) and by the European Community Research Infrastructure Integrating Activity "Study of Strongly Interacting Matter" (HadronPhysics2, Grant Agreement No. 227431) under the Seventh Framework Programme of EU. H.W. would like to thank the Kyushu University and Triangle Universities Nuclear Laboratory for hospitality and support during his stay in both institutions. We thank Professor E. Epelbaum for the insight into the present-day status of isospin breaking for chiral nuclear forces. The numerical calculations were performed on the supercomputer cluster of the JSC, Jülich, Germany.

[1] J. R. Bergervoet, P. C. vanCampen, R. A. M. Klomp, J. L. deKok, T. A. Rijken, V. G. J. Stoks, and J. J. deSwart, Phys. Rev. C **41**, 1435 (1990).
[2] V. G. J. Stoks, R. A. M. Klomp, M. C. M. Rentmeester, and J. J. deSwart, Phys. Rev. C **48**, 792 (1993).
[3] W. Glöckle, H. Witała, D. Hüber, H. Kamada, and J. Golak, Phys. Rep. **274**, 107 (1996).
[4] A. Siepe *et al.*, Phys. Rev. C **65**, 034010 (2002).
[5] X. C. Ruan *et al.*, Phys. Rev. C **75**, 057001 (2007).
[6] G. Rauprich *et al.*, Nucl. Phys. A **535**, 313 (1991).
[7] H. Patberg *et al.*, Phys. Rev. C **53**, 1497 (1996).
[8] J. Zejma *et al.*, Phys. Rev. C **55**, 42 (1997).
[9] H. Witała, R. Skibiński, J. Golak, and W. Glöckle, Eur. Phys. J. A **41**, 385 (2009).
[10] H. Witała and W. Glöckle, J. Phys. G **37**, 064003 (2010).
[11] J. Kuroś-Żołnierczuk, H. Witała, J. Golak, H. Kamada, A. Nogga, R. Skibiński, and W. Glöckle, Phys. Rev. C **66**, 024004 (2002).
[12] H. Witała, W. Glöckle, and Th. Cornelius, Few-Body Syst. **6**, 79 (1989).
[13] R. Machleidt, F. Sammarruca, and Y. Song, Phys. Rev. C **53**, R1483 (1996).
[14] V. G. J. Stoks, R. A. M. Klomp, C. P. F. Terheggen, and J. J. deSwart, Phys. Rev. C **49**, 2950 (1994).
[15] S. A. Coon *et al.*, Nucl. Phys. A **317**, 242 (1979); S. A. Coon and W. Glöckle, Phys. Rev. C **23**, 1790 (1981).
[16] S. A. Coon and H. K. Han, Few-Body Syst. **30**, 131 (2001).
[17] E. Epelbaum *et al.*, Nucl. Phys. A **671**, 295 (2000).
[18] E. Epelbaum, Prog. Part. Nucl. Phys. **57**, 654 (2006).
[19] E. Epelbaum (private communication).
[20] S. C. Pieper, Phys. Rev. Lett. **90**, 252501 (2003).
[21] W. Tornow, R. T. Braun, H. Witała, and N. Koori, Phys. Rev. C **54**, 42 (1996).

[22] W. von Witsch, X. Ruan, and H. Witała, Phys. Rev. C **74**, 014001 (2006).
[23] B. Blankleider and R. M. Woloshyn, Phys. Rev. C **29**, 538 (1984).
[24] J. L. Friar, B. F. Gibson, G. L. Payne, A. M. Bernstein, and T. E. Chupp, Phys. Rev. C **42**, 2310 (1990).
[25] R. B. Wiringa, V. G. J. Stoks, and R. Schiavilla, Phys. Rev. C **51**, 38 (1995).
[26] J. Golak, R. Skibiński, H. Witała, W. Glöckle, A. Nogga, and H. Kamada, Phys. Rep. **415**, 89 (2005).
[27] N. Kaiser, Phys. Rev. C **73**, 064003 (2006).
[28] E. Epelbaum (private communication).